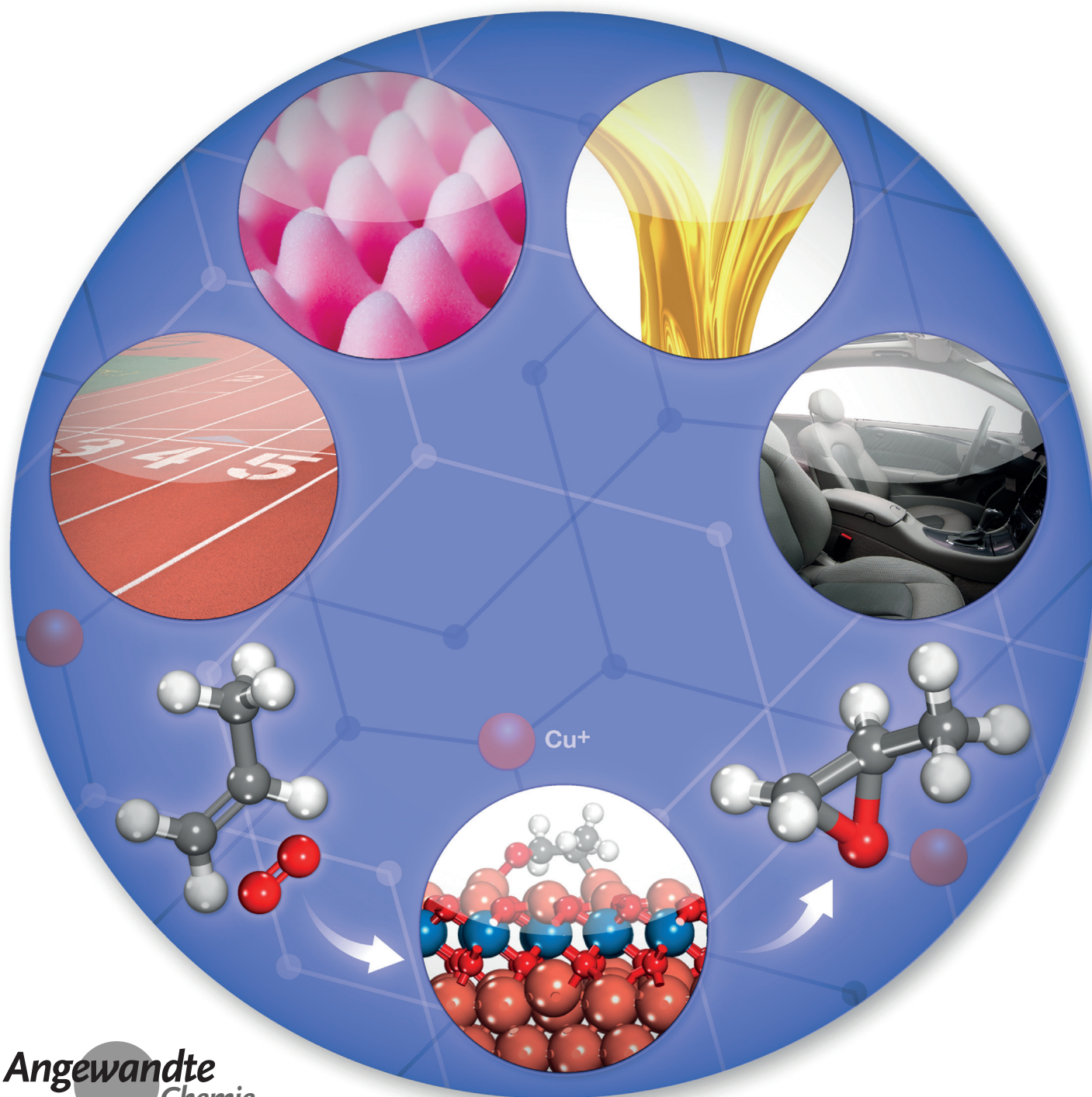




# Direct Epoxidation of Propylene over Stabilized $\text{Cu}^+$ Surface Sites on Titanium-Modified $\text{Cu}_2\text{O}$

Xiaofang Yang, Shyam Kattel, Ke Xiong, Kumudu Mudiyansele, Sergei Rykov, Sanjaya D. Senanayake, José A. Rodriguez, Ping Liu, Dario J. Stacchiola, and Jingguang G. Chen\*



**Abstract:** Direct propylene epoxidation by  $O_2$  is a challenging reaction because of the strong tendency for complete combustion. Results from the current study demonstrate that by generating highly dispersed and stabilized  $Cu^+$  active sites in a  $TiCuO_x$  mixed oxide the epoxidation selectivity can be tuned. The  $TiCuO_x$  surface anchors the key surface intermediate, an oxametallacycle, leading to higher selectivity for epoxidation of propylene.

**P**ropylene oxide (PO) is an important precursor largely produced for manufacturing numerous commodity chemicals (e.g. polyurethane and polyols). Current industrial production of propylene oxide is mainly through the chlorohydrin process and hydroperoxide mediated process, which are neither cost effective nor environmentally friendly because of generating chlorinated or peroxy-carboxylic waste.<sup>[1]</sup> Thus, identifying appropriate catalysts for direct and selective epoxidation of propylene with molecular oxygen ( $C_3H_6 + 1/2 O_2 \rightarrow C_3H_6O$ ) has received considerable attention.<sup>[2–9]</sup> For example, Au nanoparticles supported on  $TiO_2$  or titanium silicalite zeolites exhibit high selectivity (> 90%) for PO.<sup>[4]</sup> However, this approach requires co-feeding of large amount of  $H_2$  and is limited by low conversion. In contrast to ethylene epoxidation utilizing Ag-based catalysts, at present industrial-scale heterogeneous catalytic propylene epoxidation process with  $O_2$  has not been successfully developed.

The main challenge for direct propylene epoxidation with  $O_2$  is that instead of partial oxidation, propylene is readily oxidized to generate  $CO_2$  and  $H_2O$ . Some attempts have been made to improve the selectivity for PO, that is, reducing the Ag catalysts to an extremely small size (three atoms of silver),<sup>[10]</sup> or illuminating copper oxide catalysts with visible light to reduce Cu oxide during reaction.<sup>[11]</sup> Even though those studies have provided interesting approaches to alter the selectivity for epoxidation, they may not yet be practical or effective enough to be applied in large scale production. More effort is still needed to search for novel oxidation catalysts that are stable, economic, and active with significantly enhanced selectivity to the desirable epoxidation product.

Identifying surface intermediates is a critical step to understand the reaction mechanism as the surface chemistry of intermediates governs the epoxidation reaction pathway. For instance, one of the most important intermediates for ethylene epoxidation has been identified as an ethylene oxametallacycle, which has an asymmetric ring structure with one carbon atom binding directly to the surface and the second carbon atom indirectly binding to the surface through an oxygen bridge.<sup>[6,12,13]</sup> Similarly, propylene oxametallacycle has been proposed as the reaction intermediate for propylene epoxidation.<sup>[14]</sup> Even though these two oxametallacycle intermediates have a nearly identical structure, the surface chemistry of them is significantly different, resulting in different activity and selectivity. Specifically, the  $\gamma$ -hydrogen in the propylene oxametallacycle is very active and readily reacts with surface oxygen, leading to dehydrogenation and finally complete oxidation of the allyl species. The formation of the propylene oxametallacycle intermediate has been attributed to the higher selectivity for epoxidation on the copper surface.<sup>[14]</sup> However, the activity of Cu catalysts is low with a conversion of less than 4% at below 300 °C<sup>[15]</sup> and deactivation occurs because of the complete oxidation of copper to  $Cu^{2+}$ .<sup>[11]</sup> Thus, it is important to improve the activity by stabilizing Cu in low oxidation states under the reaction conditions.

Mixed oxides, such as spinels or perovskites, are stable, highly ordered, and are characterized by their unique electronic structure and physical/chemical properties.<sup>[16]</sup> Thus, they have become the focus of numerous research efforts related to catalytic oxidation reactions.<sup>[17]</sup> For instance, a mixed oxide made of  $TiCuO_x$  demonstrates high catalytic activity for CO oxidation with copper being stabilized as  $Cu^+$ .<sup>[18]</sup> The stabilization of  $Cu^+$  by  $TiO_x$  strongly suggests that  $TiCuO_x$  may show promising selectivity for propylene epoxidation. By stabilizing and controlling the density of the surface  $Cu^+$  sites,  $TiCuO_x$  may act as a potential candidate for catalyzing direct propylene epoxidation. To test this hypothesis, in this study a model Ti–Cu oxide catalyst grown on Cu(111) has been prepared by physical vapor deposition and its catalytic performance for direct propylene epoxidation is measured by temperature-programmed desorption (TPD). The adsorption of propylene oxide and the formation of oxametallacycle have been also studied by soft X-ray photo-emission spectroscopy (XPS) and high-resolution electron energy loss spectroscopy (HREELS). This study shows that the model catalysts are active and selective for converting propylene into propylene oxide by direct partial oxidation, illustrating the importance of forming stable  $Cu^+$  sites in controlling the epoxidation activity and selectivity.

The  $TiCuO_x$  thin film was synthesized by depositing Ti oxide onto a  $Cu_2O$  surface and annealing under an  $O_2$  environment. The  $Cu_2O$  surface was prepared by annealing a Cu(111) in  $O_2$  at 650 K.<sup>[19]</sup> Deposition of  $TiO_x$  causes formation of both  $TiO_2$  hexagonal islands and Ti modified row structures. Figure 1 A shows the high-resolution STM image of the surface structure with the Ti-rich regions showing depressions. The detailed structure of this  $TiCuO_x$  thin film has been described in a previous paper<sup>[18]</sup> and the STM images with large area are shown in the Supporting Information

[\*] Dr. X. Yang, Dr. S. Kattel, Dr. K. Mudiyansele, Dr. S. D. Senanayake, Dr. J. A. Rodriguez, Dr. P. Liu, Dr. D. J. Stacchiola, Prof. Dr. J. G. Chen  
Chemistry Department  
Brookhaven National Laboratory  
2 Center St., Upton, NY 11973 (USA)  
K. Xiong  
Department of Chemical and Biomolecular Engineering, University of Delaware, 150 Academy St., Newark, DE 19716 (USA)  
Dr. S. Rykov  
Sergei Rykov, Department of Semiconductors Physics and Nano-electronics, Peter the Great St. Petersburg Polytechnic University  
195251 St. Petersburg (Russia)  
Prof. Dr. J. G. Chen  
Department of Chemical Engineering  
Columbia University  
500 W. 120th St., New York, NY 10027 (USA)  
E-mail: jgchen@columbia.edu

Supporting information for this article is available on the WWW under <http://dx.doi.org/10.1002/anie.201504538>.



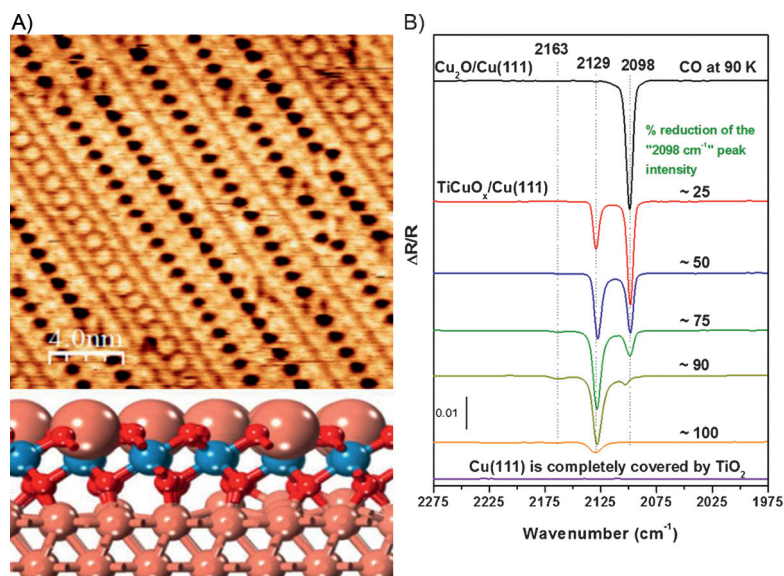


**Figure 1.** Surface structures of TiCuO<sub>x</sub> and CO adsorption. A) Atornically resolved STM images of TiCuO<sub>x</sub> and corresponding DFT simulated surface structures (O red, Ti blue, and Cu reddish-orange). Cu atoms in surface layers are enlarged. B) IRRAS after CO adsorption on TiO<sub>x</sub> modified surfaces. Peak assignments: 2098 cm<sup>-1</sup> CO on Cu<sub>2</sub>O, 2163 cm<sup>-1</sup> CO on TiO<sub>2</sub>, 2129 cm<sup>-1</sup> CO on TiCuO<sub>x</sub>.

(Figure S1). The structural study by atornically resolved STM images, near-edge X-ray absorption fine structure (NEXAFS) measurements, CO titration with infrared reflection absorption spectroscopy (IRRAS) and density functional theory (DFT) simulations confirmed the formation of mixed oxide, TiCuO<sub>x</sub>. This surface demonstrated large enhancement for CO oxidation and superior chemical stability than Cu<sub>2</sub>O because of the stabilization of Cu<sup>+</sup> by TiO<sub>x</sub>.<sup>[18]</sup> CO has been used as a probe molecule to further characterize the nature of the surface Cu sites and the results are shown in Figure 1B. New active sites for binding CO with the IR peak at 2129 cm<sup>-1</sup> were created after submonolayer TiO<sub>x</sub> modification, corresponding to the creation of the Cu<sup>+</sup> sites. The ability of the surface Cu<sup>+</sup> sites to oxidize CO demonstrates a facile dissociation of O<sub>2</sub>, an ability that may extend to other oxidation reactions, such as olefin epoxidation.

The formation of the propylene oxametallacycle intermediate has been proposed as the key step in the propylene epoxidation reaction.<sup>[14]</sup> Thus, to examine if the mixed oxide surface of TiCuO<sub>x</sub> exhibits catalytic activity for epoxidation, PO was adsorbed as a probe molecule on the surface and the resulting surface species were investigated by TPD, XPS, and HREELS. Identification of the energy loss peaks in HREELS was assisted by DFT calculations. As a comparison, similar PO adsorption experiments on both Cu(111) and Cu<sub>2</sub>O surfaces were performed under two different adsorption temperatures, 110 K and 210 K. The full comparison and discussion of the TPD, XPS, and HREELS results on all three surfaces are provided in the Supporting Information.

As shown in Figure 2, low temperature (110 K) adsorption on both Cu(111) and Cu<sub>2</sub>O results in all PO molecules desorbing at approximately 150 K, indicating weakly bound PO. A different TPD profile with a broad tail extending from 120 to 320 K is observed for the TiCuO<sub>x</sub> surface. Most PO still

weakly binds to the TiCuO<sub>x</sub> surface after adsorption at low temperatures. However, the tail between 250 and 320 K suggests stronger bonding to the surfaces. This strong-bonding feature can be more readily observed after exposing PO on the TiCuO<sub>x</sub> surface at 210 K. Large desorption peaks of PO appears at 200–330 K and the overall intensity is much larger than that desorbed from both Cu(111) and Cu<sub>2</sub>O surfaces in the same temperature range. The lower amount of PO desorption from both Cu(111) and Cu<sub>2</sub>O surfaces is due to the PO decomposition at 210 K, as shown in the comparison of the XPS results in the Supporting Information (Figure S2). Increasing the load of Ti on the Cu<sub>2</sub>O surface causes the formation of large TiO<sub>x</sub> islands.<sup>[18]</sup> PO has less tendency to bind these TiO<sub>x</sub> islands as shown by the results in Figure 2D in which less PO desorption is observed from a TiCuO<sub>x</sub> surface with higher Ti coverages (0.9 ML).

The C1s XPS spectra have been found to be useful in identifying the oxametallacycle intermediate for ethylene epoxidation.<sup>[6]</sup> In our study, C1s and O1s were recorded after PO was

adsorbed at both 110 and 210 K on all three surfaces. Figure 3A shows the XPS spectra after adsorption of PO on TiCuO<sub>x</sub>; complete comparisons of the XPS spectra after PO adsorption are provided in the Supporting Information (Figure S2). The C1s spectra after PO adsorption on these

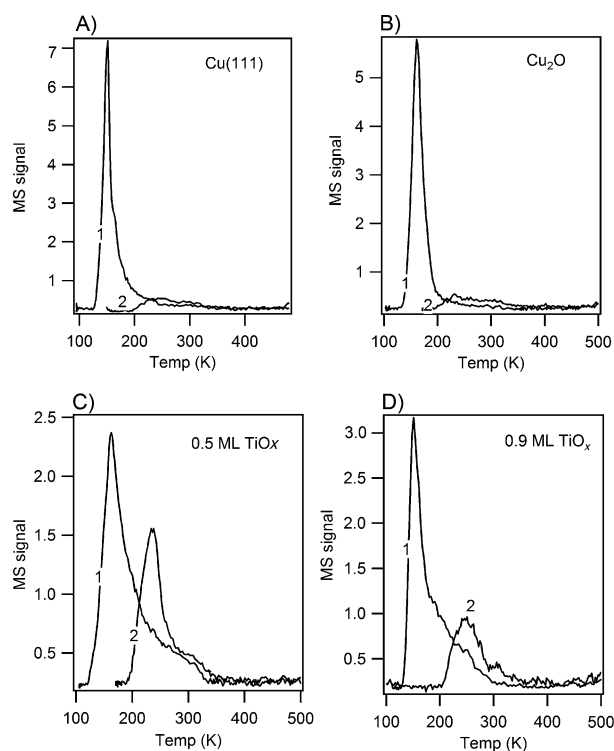


**Figure 2.** Propylene oxide (PO) TPDs after the adsorption of PO on A) Cu(111), B) Cu<sub>2</sub>O/Cu(111), and C) TiCuO<sub>x</sub> surfaces with 0.5 monolayer (ML) and D) 0.9 ML of TiO<sub>x</sub> at 1) 110 K and 2) 210 K. *m/e* = 58.

surfaces at 110 K are essentially equivalent. After deconvolution, two peaks with the binding energy (BE) at 285.6 eV and 286.8 eV are displayed with an intensity ratio of approximate 1:2 (Figure 3A), which is the expected carbon ratio of the methyl group to the methylene group in the PO molecule. Thus, XPS results indicate that the epoxide ring remains intact at low temperatures and PO most likely weakly binds to the surface through the O atom.

Different C1s features were obtained after PO adsorption on  $\text{TiCuO}_x$  at 210 K. As shown in Figure 3A, the C1s peak positions shift to slightly higher binding energy (0.2–0.4 eV). For such small shifts in binding energy, the assignment of these two peaks is similar to that of the physisorbed PO. Specifically, the peak at 285.8 eV is due to the carbon not directly bound to oxygen (C–CH<sub>3</sub>) while the peak at 287.2 eV is assigned to the carbon directly bound to oxygen (C–O). However, the relative peak intensities at 285.8 and 287.2 eV are almost reversed with the larger peak at 285.8 eV indicating that exposure to PO at 210 K results in a different

adsorption geometry for PO on  $\text{TiCuO}_x$ . One possible surface species that formed at 210 K is an oxametallacycle.

To confirm the presence of the oxametallacycle intermediate, the surface species formed after PO adsorption has been further studied by HREELS and DFT calculations (Figure 3B,C). As shown in the Supporting Information (Figure S3), low-temperature (110 K) adsorption of PO produces very similar HREELS spectra for all the surfaces. The assignments of the peaks are summarized in Table S1. The HREELS peak at 805 cm<sup>-1</sup> is assigned to the C–C–O ring deformation and the presence of this peak indicates that PO is only weakly adsorbed without opening of the ring. Different HREELS spectra are obtained after the PO adsorption at 210 K. The peak at 805 cm<sup>-1</sup> completely disappears on the Cu(111) and Cu<sub>2</sub>O surfaces. More importantly, shifting of the peak from 805 to 899 cm<sup>-1</sup> and the appearance of a new peak at 705 cm<sup>-1</sup> are observed on the  $\text{TiCuO}_x$  surface. To gain further insights into the new peaks observed at higher temperatures, DFT calculations are performed to obtain the optimized geometries for PO and oxametallacycle adsorption on the Cu<sub>2</sub>TiO<sub>3</sub> monolayer supported on Cu(111). As shown in Figure 3C, both PO and the oxametallacycle prefers the Cu<sup>+</sup> sites in a  $\eta^1$  and a  $\eta^2$  conformation, respectively. In both cases the Cu<sup>+</sup> is pulled out of the surface in interaction with the adsorbate, which enhances the adsorbate–surface binding. In general, the DFT calculated vibrational frequencies match very well with experimental HREELS measurements, strongly indicating the presence of the propylene oxametallacycle on the  $\text{TiCuO}_x$  surface. However, this intermediate is not present on either Cu(111) or Cu<sub>2</sub>O surfaces after PO adsorption (Figure S3).

Overall, the combined results from TPD, XPS, and HREELS provide strong evidence that PO is chemically adsorbed on the  $\text{TiCuO}_x$  surface to form the propylene oxametallacycle intermediate and then thermally desorbs as molecular PO by ring closing upon heating. Generating this di- $\sigma$ -bonded oxametallacycle is critically important for catalyzing the direct propylene epoxidation. For example, improved selectivity to PO has been achieved on highly dispersed Ag catalysts because they have suitable electronic and geometric properties for anchoring this oxametallacycle intermediate.<sup>[10,20]</sup> Similarly, the presence of the oxametallacycle intermediate on  $\text{TiCuO}_x$  suggests the possibility of propylene epoxidation over this surface. To test this hypothesis, direct propylene epoxidation catalyzed by the  $\text{TiCuO}_x$  surface was explored and compared to the results on Cu(111) and Cu<sub>2</sub>O surfaces under low pressure conditions.

Figure 4 shows the TPD results after co-exposing O<sub>2</sub> and propylene at 240 K. The possible products and their main *m/e* cracking patterns (in parentheses) from propylene oxidation are CO<sub>2</sub> (44), H<sub>2</sub>O (18), acetone (58, 43), propanal (58, 57), propylene oxide (58, 43, 31), and acrolein (56). Propanal can be excluded as no ion with *m/e* 57 was detected. The amounts of CO<sub>2</sub> and H<sub>2</sub>O generated through complete combustion are also negligible (see Figure S4). Thus, the major desorption products are propylene oxide, acetone, and acrolein. The quantification of each product is based on the analysis of the desorption peak areas of *m/e* 58, 56, 43, and 31, as described in the Supporting Information. Figure 4B shows

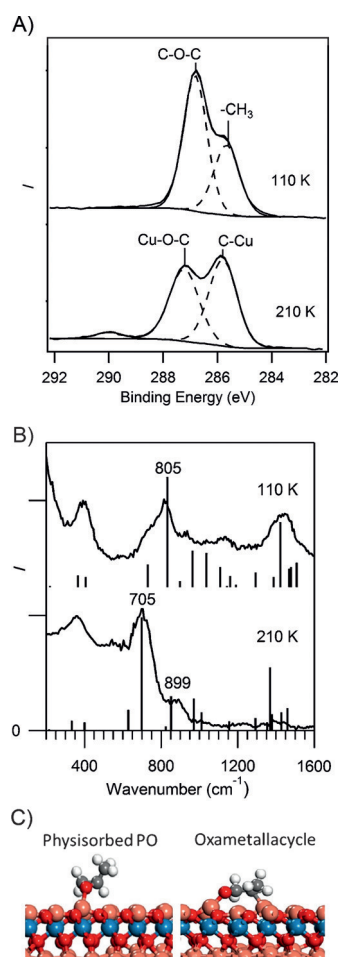


**Figure 3.** Identification of propylene oxametallacycle after PO adsorption on  $\text{TiCuO}_x$ . A) XPS of adsorbed PO at both 110 K and 210 K. B) HREELS of adsorbed PO at 110 K and 210 K, and DFT calculated vibrational frequencies (vertical lines) of adsorbed PO and oxametallacycle. C) DFT Optimized PO and oxametallacycle adsorption configurations on  $\text{TiCuO}_x$  (O red, Ti blue, Cu reddish-orange, C gray, and H white).

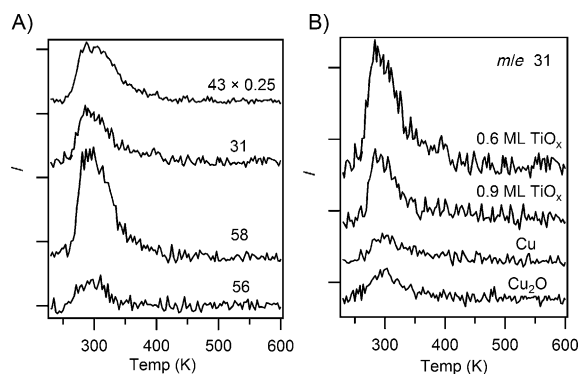


**Figure 4.** TPD of propylene epoxidation. A) Catalytic activity of  $\text{TiCuO}_x$  for the  $m/e$  values indicated next to the traces.  $\times 0.25$  is the re-scaling factor for the  $m/e = 43$  peak for better view. B) of  $\text{Cu}(111)$ ,  $\text{Cu}_2\text{O}$ , and  $\text{TiCuO}_x$  (with 0.9 and 0.6 ML of  $\text{TiO}_x$ ) in PO production ( $m/e$  31).  $\text{O}_2$ :  $1.0 \times 10^{-6}$  Torr, propylene:  $1.0 \times 10^{-6}$  Torr, 240 K for 60 min. Heating rate:  $3 \text{ K s}^{-1}$ . Plots vertically offset for clarity.

the production of propylene oxide ( $m/e$  31) among the four surfaces:  $\text{Cu}(111)$ ,  $\text{Cu}_2\text{O}$ , and  $\text{TiCuO}_x$  surfaces with 0.6 ML and 0.9 ML  $\text{TiO}_x$ . The  $\text{TiCuO}_x$  surfaces exhibit higher activity than  $\text{Cu}(111)$  or  $\text{Cu}_2\text{O}$ , with the highest activity (corresponding to 0.037 ML PO) from the 0.6 ML  $\text{TiO}_x$  surface. On  $\text{TiCuO}_x$  the calculated selectivity is 69.0% for PO, 12.7% for acetone, and 18.3% for acrolein, indicating that the  $\text{TiCuO}_x$  surface is active and selective for propylene epoxidation.

Surface-oxygen basicity or nucleophilicity is considered as an important factor to determine the selectivity in both ethylene and propylene epoxidation.<sup>[14,21]</sup> It has been proposed as a source for the different catalytic activity between copper and silver. For example, oxygen bonded to silver is more basic than oxygen bonded to copper. Consequently, silver favors allylic hydrogen stripping but copper favors stable metallacycle formation. Thus, to improve the selectivity for PO, the basicity (nucleophilicity) of the surface oxygen in the oxide should be decreased.<sup>[21]</sup> Largely different from the facile reduction of  $\text{Cu}_2\text{O}$  by low-pressure  $\text{CO}$ ,<sup>[19,22]</sup> the  $\text{TiCuO}_x$  surface cannot be reduced by  $\text{CO}$  under the same conditions, suggesting the basicity of the mixed oxide is lower than in  $\text{Cu}_2\text{O}$ .<sup>[18]</sup> Modification of  $\text{Cu}_2\text{O}$  by  $\text{TiO}_2$  appears to be an effective way to both stabilize the  $\text{Cu}^+$  and decrease the basicity of oxide, making  $\text{TiCuO}_x$  a promising catalyst for propylene epoxidation.

In summary, a model mixed oxide thin film formed by adding  $\text{TiO}_x$  to a  $\text{Cu}_2\text{O}$  surface has been explored for the direct epoxidation of propylene. The extent of propylene epoxidation on the three surfaces is well correlated with that for the oxametallacycle formation after exposing PO at 210 K, strongly suggesting that the capability to form the oxametallacycle species is a key factor for propylene epoxidation. The  $\text{TiCuO}_x$  oxide can effectively stabilize surface  $\text{Cu}^+$  and is ideal for anchoring the key surface intermediate, an oxametallacycle, leading to higher selectivity for the epoxidation of propylene. The strategy of forming stable mixed oxides could lead to a simple method in catalyst preparation and flexibility in controlling the selectivity. Results from the current study demonstrate the potential to synthesize mixed metal oxides

with stabilized  $\text{Cu}^+$  sites, which could improve the future production of PO by direct propylene oxidation.

## Experimental Section

Samples were prepared and characterized in a UHV-system equipped with STM at BNL. HREELS was obtained at Columbia University. An Omicron STM was used to obtain room temperature images of mixed oxides,  $\text{TiCuO}_x$ . XPS was performed at beamline U12a in NSLS at incident energy of ca. 400 eV at an energy resolution of 0.3 eV. IRRAS studies were carried out with a Nicolet Nexus 670 Fourier-transform infrared (FTIR) at BNL. Further details of the methods are provided in the Supporting Information.

## Acknowledgements

The work was sponsored by the U.S. Department of Energy, Office of Science under Contract No. DE-AC02-98CH10886. This research used resources of the Center for Functional Nanomaterials and National Synchrotron Light Source, which are U.S. DOE Office of Science User Facilities at Brookhaven National Laboratory under Contract No. DE-SC0012704 and the National Energy Research Scientific Computing Center (NERSC) supported by the Office of Science of the U.S DOE under Contract No. DE-AC02-05CH11231.

**Keywords:** copper · epoxidation · mixed oxides · oxidation · propylene oxide

**How to cite:** *Angew. Chem. Int. Ed.* **2015**, *54*, 11946–11951  
*Angew. Chem.* **2015**, *127*, 12114–12119

- [1] T. A. Nijhuis, M. Makkee, J. A. Moulijn, B. M. Weckhuysen, *Ind. Eng. Chem. Res.* **2006**, *45*, 3447–3459.
- [2] Y. Pang, X. Chen, C. Xu, Y. Lei, K. Wei, *ChemCatChem* **2014**, *6*, 876–884.
- [3] X. Zuwei, Z. Ning, S. Yu, L. Kunlan, *Science* **2001**, *292*, 1139–1141.
- [4] T. Hayashi, K. Tanaka, M. Haruta, *J. Catal.* **1998**, *178*, 566–575.
- [5] S. Lee, L. M. Molina, M. J. López, J. A. Alonso, B. Hammer, B. Lee, S. Seifert, R. E. Winans, J. W. Elam, M. J. Pellin, S. Vajda, *Angew. Chem. Int. Ed.* **2009**, *48*, 1467–1471; *Angew. Chem.* **2009**, *121*, 1495–1499.
- [6] S. Linic, H. Piao, K. Adib, M. A. Barteau, *Angew. Chem. Int. Ed.* **2004**, *43*, 2918–2921; *Angew. Chem.* **2004**, *116*, 2978–2981.
- [7] M. Ojeda, E. Iglesia, *Chem. Commun.* **2009**, 352–354.
- [8] B. Chowdhury, J. J. Bravo-Suárez, M. Daté, S. Tsubota, M. Haruta, *Angew. Chem. Int. Ed.* **2006**, *45*, 412–415; *Angew. Chem.* **2006**, *118*, 426–429.
- [9] Q. Hua, T. Cao, X.-K. Gu, J. Lu, Z. Jiang, X. Pan, L. Luo, W.-X. Li, W. Huang, *Angew. Chem. Int. Ed.* **2014**, *53*, 4856–4861; *Angew. Chem.* **2014**, *126*, 4956–4961.
- [10] Y. Lei, F. Mehmood, S. Lee, J. Greeley, B. Lee, S. Seifert, R. E. Winans, J. W. Elam, R. J. Meyer, P. C. Redfern, D. Teschner, R. Schlögl, M. J. Pellin, L. A. Curtiss, S. Vajda, *Science* **2010**, *328*, 224–228.
- [11] A. Marimuthu, J. Zhang, S. Linic, *Science* **2013**, *339*, 1590–1593.
- [12] J. W. Medlin, M. A. Barteau, *J. Phys. Chem. B* **2001**, *105*, 10054–10061.
- [13] J. W. Medlin, M. A. Barteau, J. M. Vohs, *J. Mol. Catal. A* **2000**, *163*, 129–145.
- [14] D. Torres, N. Lopez, F. Illas, R. M. Lambert, *Angew. Chem. Int. Ed.* **2007**, *46*, 2055–2058; *Angew. Chem.* **2007**, *119*, 2101–2104.

- [15] O. P. H. Vaughan, G. Kyriakou, N. Macleod, M. Tikhov, R. M. Lambert, *J. Catal.* **2005**, *236*, 401–404.
- [16] M. A. Peña, J. L. G. Fierro, *Chem. Rev.* **2001**, *101*, 1981–2018.
- [17] I. E. Wachs, K. Routray, *ACS Catal.* **2012**, *2*, 1235–1246.
- [18] A. E. Baber, X. Yang, H. Y. Kim, K. Mudiyansele, M. Soldemo, J. Weissenrieder, S. D. Senanayake, A. Al-Mahboob, J. T. Sadowski, J. Evans, J. A. Rodriguez, P. Liu, F. M. Hoffmann, J. G. Chen, D. J. Stacchiola, *Angew. Chem. Int. Ed.* **2014**, *53*, 5336–5340; *Angew. Chem.* **2014**, *126*, 5440–5444.
- [19] F. Yang, Y. Choi, P. Liu, J. Hrbek, J. A. Rodriguez, *J. Phys. Chem. C* **2010**, *114*, 17042–17050.
- [20] A. Takahashi, N. Hamakawa, I. Nakamura, T. Fujitani, *Appl. Catal. A* **2005**, *294*, 34–39.
- [21] T. C. R. Rocha, M. Hävecker, A. Knop-Gericke, R. Schlögl, *J. Catal.* **2014**, *312*, 12–16.
- [22] A. E. Baber, F. Xu, F. Dvorak, K. Mudiyansele, M. Soldemo, J. Weissenrieder, S. D. Senanayake, J. T. Sadowski, J. A. Rodriguez, V. Matolín, M. G. White, D. J. Stacchiola, *J. Am. Chem. Soc.* **2013**, *135*, 16781–16784.

Received: May 19, 2015

Published online: July 17, 2015